3-1-1990

Fast-wave Current Drive above the Slow-Wave Density Limit

D. P. Sheehan
University of San Diego, dsheehan@sandiego.edu

R. McWilliams
University of California, Irvine

N. S. Wolf
University of California, Irvine

D. Edrich
University of California, Irvine

Fast-Wave Current Drive above the Slow-Wave Density Limit

D. P. Sheehan,[a] R. McWilliams, N. S. Wolf,[b] and D. Edrich
Department of Physics, University of California at Irvine, Irvine, California 92717
(Received 22 May 1989)

Fast-wave and slow-wave current drive near the mean gyrofrequency were compared in the Irvine Torus. The observation of the slow-wave current-drive density limit was extended by an order of magnitude in wave frequency compared to previous tokamak results. At low densities, the fast-wave antenna was observed to launch slow waves which drove currents that suffered from a current-drive density limit identical to that for waves launched from the slow-wave antenna. At higher densities, current was driven by the fast-wave antenna while none was driven by the slow-wave antenna.

PACS numbers: 52.40.Fd, 52.50.Gj

In the lower-hybrid frequency range, two cold plasma waves—the fast and slow waves—have been investigated as promising means to drive steady-state electron currents in tokamaks. Following Fisch's[1] prediction, McWilliams *et al.* experimentally discovered slow-wave lower-hybrid current drive (LHCD)[2-4] which demonstrated current drive by both collisional and collisionless transfer of wave momentum to electrons. Perhaps the earliest tokamak LHCD experiment operating in a collisionless regime was done by Yamamoto *et al.*[5] Since then, LHCD has been investigated extensively, as summarized in Ref. 6. Despite the success of slow-wave LHCD, there remains a problem with the current-drive "density limit," a density threshold above which current-drive efficiency falls dramatically. Fast waves, on the other hand, might propagate to higher densities[7] and drive currents above the slow-wave density limit.[8] Experiments by McWilliams and Platt in the Irvine Torus[9] discovered that a phased-array fast-wave antenna could drive currents. Current drive by fast-wave toroidal eigenmode excitation and unidirectional launching from antennas designed to excite fast waves has been reported on a number of devices[10-15] including ACT-I, JFT-2M, JIPP T-IIU, PLT, and WT-3.

Despite extensive experimental and theoretical investigations of fast- and slow-wave propagation and current drive, a number of central issues remain unresolved, of which one has been the failure of fast waves in the lower-hybrid frequency range to drive currents consistently and demonstrably above the slow-wave density limit. Recent fast-wave current-drive results on JIPP T-IIU (Ref. 14) exhibit many characteristics of slow-wave current drive including the density limit. Experimentalists on JIPP T-IIU speculate that their antenna actually coupled to the slow wave, rather than to the fast wave, through parasitic excitation. Goree and Ono have demonstrated parasitic excitation of lower-hybrid slow waves by a fast-wave current-drive antenna in ACT-I.[16]

The present paper compares experimental results of fast- and slow-wave antennas under identical plasma conditions, for similar principal wavelengths, and over the same wide frequency range (rather than a single frequency), and input power levels. The new results presented here are the following: (i) Current drive was obtained with the fast-wave antenna at densities demonstrably above the slow-wave density limit. (ii) At low densities, the fast-wave antenna was observed to launch slow waves and these slow waves drove currents which suffered the same current-drive density limit as those launched from the slow-wave antenna. (iii) The slow-wave current-drive density limit was extended an order of magnitude in wave frequency over previous experiments.

The experiments were performed on the Irvine Torus ($R=55.6$ cm, $a=3.5$ cm, graphite limiter, $B_\phi=1.0$ kG), with plasma produced by electron-impact ionization.[17] There is no Ohmic pulse and, hence, no dc toroidal electric field or polodial magnetic field from Ohmic current. The present experiments were performed in helium with plasma densities $n_{e0}\leq 2\times 10^{12}$ cm^{-3} and bulk electron temperatures $T_{e0}\leq 10$ eV, using up to 3.2 A of ionizing electron-beam current at 300-V initial energy (current drive was observed with either rf antenna powered, for electron-beam bias from 150 to 350 V, the operating range of the source). The plasma density was adjusted by varying this electric current. Little or no change in electron temperature has been observed for changes in plasma density over the experimental regime. Density fluctuations increase roughly a factor of 3 from the lowest to highest densities. The torodially symmetric ionizing electron beams also provide a tail population out to about 600 V as a result of electron-beam–plasma instabilities.[17] These tail electrons provide a target population for resonant wave damping and current drive. Beam electron density to bulk electron density was typically $n_{eb}/n_{e0}\approx 10^{-2}$.

Plasma density and bulk electron temperatures were inferred from radially moveable Langmuir probes and the propagation angle of lower-hybrid waves. Wave-driven currents were measured by means of a small-area, single-turn, dual-loop probe positioned just outside the plasma and oriented to detect $\partial B_\theta/\partial t$, the time rate of

change of the induced poloidal magnetic field. The loops were arranged to discriminate against electrostatic pick-up.

The fast-wave (FW) antenna consists of sixteen independently phased elements forming an array four elements long toroidally by four elements spaced equidistantly around the plasma poloidally.[9] The slow-wave antenna consists of eight coaxial 0.6-cm-wide tantalum rings situated equidistantly toroidally outside a thin quartz tube. Similar toroidal vacuum power spectra can be launched by both fast- and slow-wave antennas. At wave frequency 100 MHz, the FW calculated vacuum principal indices of refraction were $n_\parallel = 10.0$ and $n_\theta = 13.7$ for adjacent-antenna-element phasing $\Delta\phi = \pm\pi/2$; for the slow wave, $n_\parallel = 10.0$ for phasing $\Delta\phi = \pm\pi/2$ between adjacent pairs of rings. For strong linear electron Landau damping at 100 MHz, $n_\parallel \gtrsim 5/T_e^{1/2}$ (keV) is required. For 0.3-keV electrons, $n_\parallel \approx 10$ satisfies this requirement. The antennas were excited by application of 20–200 MHz rf with variable duty cycle with typical average power of 0.5 W to the plasma, far below the zeroth-order power used to generate the plasma (up to 950 W). The rf-driven electron currents lasted for the duration of the rf pulse and, thus, are not caused by a transient effect. The rf voltage applied to the antenna elements was 1–150 V compared with 10-eV bulk electron temperatures and 300–600-V electron tail populations. For comparison, large-tokamak LHCD experiments have antenna voltages approaching 10 keV with bulk electron temperatures around 1 keV, a ratio similar to that studied in the Irvine Torus. The pulsed rf was observed to have no effect on bulk plasma densities or electron temperatures. Both antennas are designed to couple electrostatically to their respective waves; roughly 1 A current ran through individual antenna elements. The small magnitude of antenna currents and the geometry of the experimental setup precluded confusion of antenna-generated magnetic fields with fields generated by rf-induced currents. Additionally, in the absence of plasma, no probe signals were detected which might have indicated magnetic fields from either antenna or rf-driven currents.

Previous tokamak experiments[6] have studied the slow-wave LHCD density limit over one decade in launched-wave frequency. By using the slow-wave antenna, the Irvine Torus results extend these data an added order of magnitude by studying 20 MHz $\leq f \leq$ 200 MHz. As shown in Fig. 1, which displays only slow-wave-antenna results for all devices shown, the Irvine LHCD density limits follow the trend of previous tokamak results. For the present data, the slow-wave LHCD density limit was taken to be the density at which the current-drive efficiency decreases 20% from its maximum value.

Next, waves were launched from the fast-wave antenna. In slab geometry, the fast-wave propagation cutoff

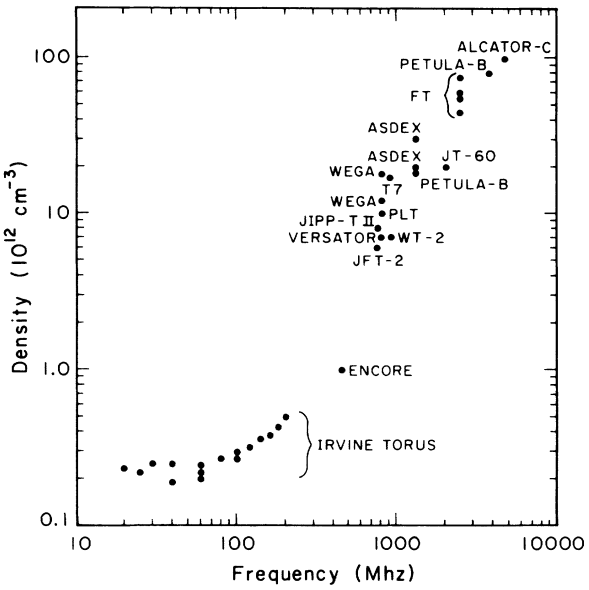

FIG. 1. Slow-wave density limit vs frequency for Irvine Torus and various tokamaks (from Ref. 6).

density is given approximately by

$$\omega_{pe}^2(\text{cutoff,FW}) \approx \omega\omega_{ce}(n_\parallel^2 + n_\theta^2 - 1)^{1/2}(n_\parallel^2 - 1)^{1/2}, \quad (1)$$

where $n_\parallel$ and n_θ are determined by the launching antenna. For cyclindrical geometry, the wave cutoff density may shift slightly. Equation (1) does provide a guideline that we might not expect to observe fast waves for densities below the high 10^{11}-cm^{-3} range. In fact, fast-wave effects were not observed for $n_e \leq 9\times10^{11}$ cm^{-3}. However, for densities below $n_e \approx 5\times10^{11}$ cm^{-3} the fast-wave antenna was observed to launch small-amplitude slow waves (SW), which have a dramatically lower cutoff density, given approximately by $\omega_{pe}^2(\text{cutoff, SW}) \approx \omega^2$.

Several fast-wave current-drive experiments unexpectedly have encountered current-drive density limits consistent with slow-wave observations. There has been speculation that the fast-wave antennas coupled primarily to slow waves in the plasma, which would give such results. The present paper reports the first experiment directly measuring the slow waves and slow-wave-driven current generated from an antenna designed to launch fast waves. For low densities in the present experiment, the fast-wave antenna couples to slow waves (identified by probe measurements) with about 10%–30% of the efficiency of the slow-wave antenna. At these low densities, the slow waves generated by the fast-wave antenna are observed to drive electron currents which are subject to the slow-wave LHCD density limit just as are slow waves launched from the slow-wave antenna. Hence, fast-wave antennas can be subject to the slow-wave LHCD density limit when the antennas are operated in

low-density plasmas. In fact, the physical construction of the fast-wave antenna[9] intuitively suggests it should couple weakly to the slow wave.

Figure 2 shows that the fast-wave antenna can generate currents at densities well above the slow-wave current-drive density limit. First, the current driven by the slow-wave antenna (excited at 100 MHz) was measured as a function of density. The slow-wave data show a density limit near 2.8×10^{11} cm^{-3}, followed by current decreasing monotonically with increased plasma density until it falls below noise levels imposed by circuitry and random electric currents in the plasma. The maximum current driven by fast and slow waves in these experiments was about 1 A. In the experimental regime, current scales roughly linearly with power, with a maximum current-drive efficiency of $\eta = InR/P \sim (6\times10^{-2}$ A/W$)(10^{-13}$ cm$^{-3})$ m. This is comparable to observations on other small-machine slow-wave current-drive experiments, an efficiency which has increased with device size in large tokamaks.

For the fast-wave and slow-wave antennas separately, it has been shown that the magnitude and direction of the driven currents depend on the phasing of the antenna array elements. When symmetric phasing was used, no current was detected. To produce current drive, the phase difference between adjacent elements was $\pm 90°$ depending on the direction desired. The current produced was slightly, but not significantly, larger for one phasing compared to the other. The direction of the induced electron flow was in the direction of the toroidal phase velocity of the launched waves.

Next, the fast-wave antenna was excited at 100 MHz. For densities below about 5×10^{11} cm^{-3} the fast-wave antenna drives currents with similar density dependence as the slow-wave antenna. Above $n_i \approx 9\times10^{11}$ cm^{-3}, coinciding roughly with the predicted fast-wave propagation cutoff density [see Eq. (1)], the FW-antenna-driven current displays a new regime of current drive. Above this density, in Fig. 2, fast-wave current drive (FWCD) is observed up to the maximum experimental operating densities. In Fig. 2, then, fast-wave-driven currents are not observed until densities of a factor of 3 greater than the slow-wave LHCD density limit are achieved. Additionally, FWCD is seen for densities up to a factor of 6.5 above the slow-wave LHCD density limit, this factor being limited by the maximum density achievable in this experiment.

Finally, the current-drive density limit for the fast-wave antenna was compared with the slow-wave antenna for 20 MHz $\leq f \leq$ 200 MHz, and the results are shown in Fig. 3. The slow-wave components launched by the fast-wave antenna (observed only for $n_e \leq 5\times10^{11}$ cm^{-3}) agree well with the slow-wave-antenna data. Below about 80 MHz, the fast wave should be cutoff from propagation and, in fact, below 80 MHz, FWCD is not observed. For 80 MHz and above, however, fast-wave current drive is observed up to the maximum operating density for this experiment. When a fast-wave current-drive density limit was not found, this is indicated by vertical arrows. Experimentally, the magnitude of fast-wave-driven current was larger at 100 MHz than at 200 MHz, which might be due to wave accessibility considerations for this experiment.

In summary, fast- and slow-wave lower-hybrid current drive (LHCD) was observed in the Irvine Torus. The slow-wave LHCD density limit has been observed for 20 MHz $\leq f \leq$ 200 MHz, extending the previous tokamak data base by an order of magnitude in wave frequency. At densities below the slow-wave LHCD density limit, a

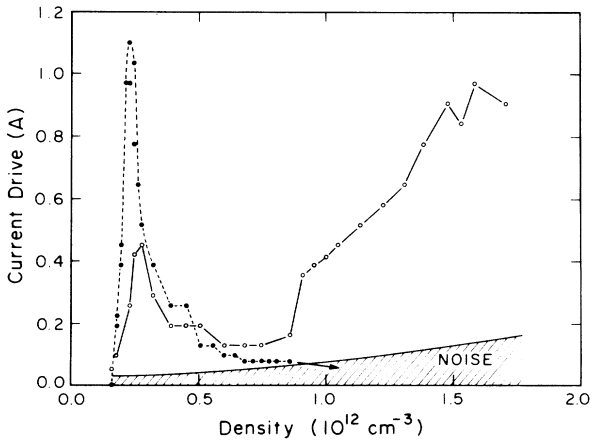

FIG. 2. Wave-driven currents by fast-wave antenna (open dots) and slow-wave antenna (solid dots) vs plasma density at 100 MHz in He plasma. Fast-wave antenna drive currents demonstrably above the slow-wave density limit.

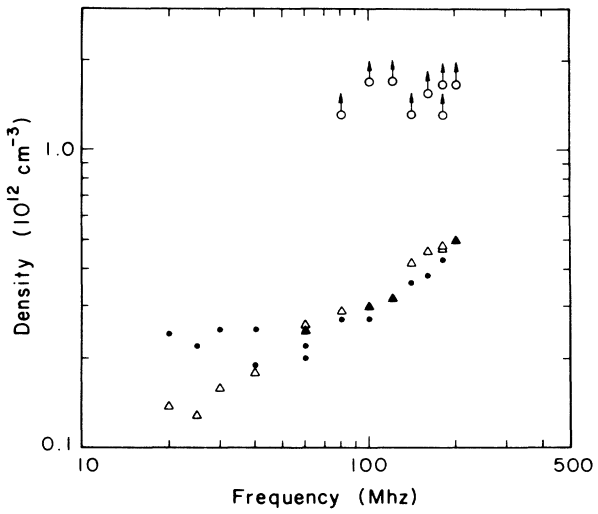

FIG. 3. Density limits vs frequency for fast- and slow-wave antennas. Solid dots: slow-wave antenna; triangles: slow-wave component launched by fast-wave antenna; open dots: fast-wave antenna. Vertical arrows indicate that no density limit was observed.

fast-wave antenna was observed to launch a fraction of power in slow waves and the attendant slow-wave LHCD density limit was observed. At densities where fast waves could propagate (which easily could require densities a factor of 3 above the observed slow-wave LHCD density limit), fast-wave driven current was observed, up to densities a factor of 6.5 above the observed slow-wave LHCD density limit. Fast-wave current drive did not encounter a density limit in these experiments. These results suggest that future tokamak fast-wave experiments should seek a different regime of operation from that used for slow-wave current drive. Subject to wave accessibility conditions, fast-wave experiments should examine densities well above the observed slow-wave current-drive density limit. Additionally, considering the initial electron tail population in the Irvine Torus and the JIPP T-IIU (Ref. 18) results, fast-wave current-drive experiments may benefit from increased electron temperatures.

It is a pleasure to thank Stacy Roe and David Parsons for valuable technical assistance. These experiments were carried out under DOE Grant NO. DE-FG03-086ER5321 and NSF Grant No. PHY 8606081.

---

[a]Permanent address: Department of Physics, University of San Diego, San Diego, CA 92110.

[b]Permanent address: Department of Physics, Dickinson College, Carlisle, PA 17013.

[1]N. J. Fisch, Phys. Rev. Lett. **41**, 873 (1978).

[2]R. McWilliams, L. Olson, R. W. Motley, and W. M. Hooke, Bull. Am. Phys. Soc. **23**, 765 (1978).

[3]R. McWilliams, E. J. Valeo, R. W. Motley, W. M. Hooke, and L. Olson, Phys. Rev. Lett. **44**, 245 (1980).

[4]R. McWilliams and R. W. Motley, Phys. Fluids **24**, 2022 (1981).

[5]T. Yamamoto *et al.*, Phys. Rev. Lett. **45**, 716 (1980).

[6]L. H. Sverdrup and P. Bellan, Phys. Rev. Lett. **59**, 1197 (1987).

[7]V. E. Golant, Zh. Tekh. Fiz. **41**, 2492 (1972) [Sov. Phys. Tech. Phys. **16**, 1980 (1972)].

[8]R. McWilliams and Y. Mok, Fusion Technol. **7**, 283 (1985).

[9]R. McWilliams and R. C. Platt, Phys. Rev. Lett. **56**, 835 (1986).

[10]J. Goree, M. Ono, P. Colestock, R. Horton, D. McNeil, and H. Park, Phys. Rev. Lett. **55**, 1669 (1985).

[11]K. Ohkubo *et al.*, Phys. Rev. Lett. **56**, 2040 (1986).

[12]R. Ando, E. Kako, Y. Ogawa, and T. Watari, Nucl. Fusion **26**, 1619 (1986).

[13]H. Tanaka *et al.*, Phys. Rev. Lett. **60**, 1033 (1988).

[14]Y. Uesugi *et al.*, in *Applications of Radio-Frequency Power to Plasmas—1987,* Proceedings of the Seventh Topical Conference, Kissimmee, FL, 1987, edited by S. Bernabei and R. W. Motley, AIP Conference Proceedings No. 159 (American Institute of Physics, New York, 1987), p. 179.

[15]R. I. Pinsker *et al.*, in *Applications of Radio-Frequency Power to Plasmas—1987* (Ref. 14), p. 175.

[16]J. Goree and M. Ono, Nucl. Fusion **28**, 1105 (1988).

[17]H. Ikuda, R. Horton, M. Ono, and K. L. Wong, Phys. Fluids **28**, 3365 (1985).

[18]T. Yamamoto *et al.*, Phys. Rev. Lett. **63**, 1148 (1989).